Aerosol Dispersion of Respirable Particles in Narrow Size Distributions Produced by Jet-Milling and Spray-Drying Techniques

Margaret D. Louey,[1,3] Michiel Van Oort,[2] and Anthony J. Hickey[1,4]

Received April 14, 2003; Accepted March 17, 2004

Purpose. To examine the effect of particle size and morphology on aerosol dispersion using jet-milled and spray-dried mannitol particles in narrow size distributions within the respirable range.

Methods. Particle size and morphology were examined by laser diffraction and scanning electron microscopy, respectively. Aerosol dispersion was examined using a cascade impactor with a preseparator operating at a flow rate of 60 L/min, using two inhaler devices: Rotahaler (low-resistance device) and Inhalator (high-resistance device). Powder flow was examined using static and dynamic methods (Carr's compressibility index and vibrating spatula, respectively).

Results. Narrow size distributions of jet-milled and spray-dried particles were produced ($d_{50\%}$ = 1.4 to 10.3 μm, GSD = 1.8 to 2.1, and $d_{50\%}$ = 1.6 to 7.5 μm; GSD = 1.5 to 1.9, respectively). All particles were highly crystalline. Differences in particle shape were observed between jet-milled and spray-dried particles. Higher fine particle fraction (FPF) and relative fine particle fraction (FPF_{rel}) (greater aerosol dispersion) and lower geometric standard deviation (GSD) (less variation) were obtained using particles with $d_{50\%}$ between 2 and 5 μm. Higher mass median aerodynamic diameter were obtained with larger $d_{50\%}$. Spray-dried particles produced greater aerosol dispersion compared with jet-milled particles. Greater aerosol dispersion was obtained using the Inhalator than the Rotahaler.

Conclusions. Small changes in the particle size within the 1–10-μm range produced a major impact in the aerosol dispersion of jet-milled and spray-dried particles. Even in these narrow size ranges, aggregation plays an important role in aerosol dispersion.

KEY WORDS: aerosol dispersion; jet-milling; narrow size distributions; respirable particles; spray-drying.

INTRODUCTION

The particle size and distribution play an important role in the aerosolization of particles. Particles with aerodynamic diameters of 1–10 μm are considered respirable (1). Very few fundamental studies have examined the relationship between particle size and aerosol dispersion, especially the transition in particle behavior in the 1- to 10-μm range. Particles in this range may be prepared by size reduction or construction techniques (2). Jet-milling is a size reduction technique whereby high-energy comminution of particles occurs by particle-particle and particle-wall collisions under the influence of opposing high-velocity jets of compressed gases. Particles prepared by jet-milling can be highly electrostatically charged, fractured crystals. Limited control over size, shape, and morphology can be exercised (3). Respirable-sized particles are traditionally prepared by jet-milling techniques. Spray-drying is a construction technique involving atomization of a liquid feed into a hot gaseous medium to produce dried particulates. Characteristics of spray-dried particles are determined by the design and operation parameters of the spray-dryer and the physical and chemical properties of the feed (4).

Few studies have examined the effect of particle size and morphology on aerosol dispersion of particles. The aerosol dispersion of different particle sizes was examined using drug alone formulations of spray-dried particles of mannitol ($d_{50\%}$ of 2.7–7.3 μm) and disodium cromoglycate (DSCG) ($d_{50\%}$ of 2.3–5.2 μm) (5,6). Lower fine particle fractions (FPF) were obtained with smaller particle sizes, attributed to higher cohesion; and at larger sizes, attributed to higher inertial impaction in the throat and upper stages. The aerosolization of jet-milled and spray-dried particles has been compared using various pharmaceutical compounds. Differences in respirable fractions were not observed between spray-dried ($d_{50\%}$ = 4.4 μm) and micronized ($d_{50\%}$ = 4.7 μm) salbutamol (albuterol) sulfate from drug alone formulations using a Spinhaler (a low resistance device) (7). Higher respirable fractions from a 1:1 drug-lactose blend was obtained from spray-dried DSCG particles ($d_{50\%}$ = 3.8 μm) than micronized DSCG particles ($d_{50\%}$ = 2.8 μm) (8). However, this difference may be the result of size differences, rather than surface morphology of DSCG particles.

The objective of this study is to examine the influence of particle size and morphology on aerosol dispersion, using jet-milled and spray-dried mannitol particles with narrow distributions in the 1–10-μm range.

MATERIALS AND METHODS

Materials

D-mannitol (ACS reagent, Sigma, St. Louis, MO, USA; lot 119H0025) was used as the model compound.

Methods

Jet-Milling

Jet-milled particles were prepared using a modified Trost GEM-T Jet-mill (Plastomer Products, Newton, NJ, USA). The size distributions were adjusted by varying the pusher pressure (30–80 psi), feed rate (slow/fast), and location of particle collection (jar, cyclone, and bag). A pressure differential of 20 psi was used for all samples.

Spray-Drying

Spray-dried particles were prepared from aqueous feed solutions using a Mini Spray-dryer B-191 (Buichi, Flawil, Switzerland) with a two-fluid nozzle. Nitrogen was used as the atomization gas. The size distributions were adjusted by varying the following parameters, as determined in a preliminary study (9): feed concentration (1–10% w/w), feed rate (2–10

[1] Drug Delivery and Disposition, School of Pharmacy, University of North Carolina, Chapel Hill, North Carolina 27599, USA.
[2] Inhalation Product Development, GlaxoSmithKline, Research Triangle Park, North Carolina 27709, USA.
[3] Current address: Inhalation Product Development, GlaxoSmithKline, Research Triangle Park, North Carolina 27709, USA.
[4] To whom correspondence should be addressed. (e-mail: ahickey@unc.edu)

0724-8741/04/0700-1200/0 © 2004 Plenum Publishing Corporation

ml/min), atomization pressure (1–3 bar), inlet temperature (120–150°C), and nozzle size (0.5–10 mm).

Analytical Method

Mannitol was quantified using a modified colorimetric assay (10). Mannitol standards or samples (0.5 ml) were placed in a glass screw-top vial, and 5 mM sodium periodate (Reagent 1) (0.25 ml) was added and mixed by vortex for 15 s at room temperature. A solution containing 0.1 M acetylacetone, 2 M ammonium acetate, and 0.02 M sodium thiosulphate (Reagent 2) (0.25 ml) was added and mixed by vortex. This mixture was heated in boiling water (100°C) for 2 min, then cooled in an ice-bath. The absorbance of the resultant yellow-colored solution was measured at a wavelength of 411 nm (UV160U UV-Visible Spectrophotometer, Shimadzu Corporation, Columbia, MD, USA). A linear range of 1–25 μg/ml was obtained ($r^2 = 0.997$) with limits of detection and quantitation determined as 1 and 2 μg/ml, respectively.

Physicochemical Characterization

The size distribution was determined by laser diffraction (HELOS Particle Size Analysis H0838, Sympatec GmbH System-Partikel-Technik, Clausthal-Zellerfeld, Germany) using the RODOS dispersing unit (40% feed rate, 4 bar pressure differential). The median diameter ($d_{50\%}$) and geometric standard deviation (GSD) was determined.

The surface morphology was examined by scanning electron microscopy (SEM) (JSM-6300 FV, JEOL, Peabody, MA, USA). Samples were attached to sample stubs using double-sided tape, then sputter coated with gold palladium alloy (Polaron 5200, Polaron Instruments, Agawan, MA) and viewed using an accelerating voltage of 15 kilovolt (kV).

The thermal properties were analyzed using differential scanning calorimetry (DSC) (DSC2010 Differential Scanning Calorimeter, TA Instruments, New Castle, DE, USA) in the range 30–200°C under a nitrogen gas purge (heating rate of 10°C/min). The onset and peak temperatures and enthalpy of transition (ΔH) were determined for each peak.

The weight loss on heating was analyzed by thermogravimetric analysis (TGA) (Hi-Res TGA2950 Thermogravimetric Analyser, TA Instruments) in the range 30–150°C with a scanning rate of 10°C/min, under a nitrogen purge. The weight loss on heating was expressed as a percentage of the initial weight.

The crystallinity was examined by X-ray diffraction (XDS2000 Diffractometer, Scintag Inc., Sunnydale, CA) in angular increments of 0.03° between the range of 2° and 50°, at a scan rate of 1°2θ/min. Samples were dusted onto a petroleum-coated quartz zero background plate.

Powder Flow

The static powder flow was characterized using Carr's compressibility index (CI), determined from the tapped (ρ_{tap}) and bulk densities (ρ_{bulk}):

$$CI = \frac{\rho_{tap} - \rho_{bulk}}{\rho_{tap}} \times 100\% \quad (1)$$

The tapped and bulk densities were measured in a 2.5-ml glass syringe (Hamilton Company, Reno, NV, USA) using an automatic tapper (Vanderkamp tap density tester, VanKel Industries Inc, Cary, NC, USA). The tapped density was determined after 2500 taps, unless otherwise stated. Lower CI values are indicative of better flow behavior.

The dynamic powder flow was characterized using a vibrating spatula method (Mettler LV3, Mettler-Toledo, Columbus, OH) (11,12). The mass of powder falling from the vibrating spatula was measured as a function of time. Measurements were performed in triplicate. Analysis of the mass vs. time profile was performed with various stride lengths to produce a Richardson plot, the logarithm of the curve length plotted as a function of the logarithm of stride length. The fractal dimension (δ) was determined from the linear part of the Richardson plot using the equation $\delta = 1 + |m|$, where m was the slope of the curve. Lower values being indicative of more regular flow behavior.

Aerosol Dispersion Characterization

The *in vitro* aerosol dispersion was determined using an eight stage, nonviable cascade impactor with a preseparator (Graseby-Andersen, Smyrna, GA, USA) operating at an airflow rate of 60 L/min. The cutoff diameters for the Andersen cascade impactor have been determined for various flow rates (13). The impaction plates were pre-coated with a 1% w/v solution of silicon oil in hexane and the preseparator contained 10 ml of purified water to prevent particle bounce and re-entrainment. Two inhaler devices were used: a low-resistance device (Rotahaler, GlaxoSmithKline, Research Triangle Park, NC, USA) and a high-resistance device (Inhalator, Boehringer Ingelheim, Ingelheim, Germany). Mannitol particles (20mg) were loaded into hard gelatin capsules (size 3, Eli Lily and Co., Indianapolis, IN, USA). A single capsule was used for each impaction with each capsule had air drawn through it for 10 s. Measurements were performed in triplicate. The amounts of mannitol remaining in the capsule and inhaler device and deposited in the throat, preseparator, individual impaction plates, and stages were quantified. The temperature and relative humidity of the surrounding environment was measured prior to each impaction.

The emitted dose (ED) was defined as the mass of particles delivered from the inhaler (i.e., total amount excluding the inhaler device and capsule), expressed as a percentage of the total amount of mannitol collected. The fine particle fraction (FPF) was defined as the mass of particles deposited in stage 2 and lower ($d_{ae} < 4$ μm), expressed as a percentage of the total amount of mannitol collected. The mass median aerodynamic diameter (MMAD) was calculated as the 50th percentile of the aerodynamic particle size distribution by mass. The geometric standard deviation (GSD) was calculated as the ratio of the particle size at the 84th percentile to the 50th percentile. Both MMAD and GSD were determined from the linear region of the plot (between the 16th and 84th percentiles) of the cumulative mass distribution as a function of the logarithm of aerodynamic diameter.

In addition, the relative fine particle fraction (FPF_{rel}) was defined as the mass of dispersed particles with $d_{ae} < 4$ μm (particles deposited in stage 2 and lower), expressed as a percentage of the total mass particles with $d_{ae} < 4$ μm. The total mass of particles with $d_{ae} < 4$ μm in each sample was estimated graphically from the laser diffraction data, assuming that primary particles were measured by the laser diffraction technique used. The equivalent diameter corresponding to d_{ae} of 4 μm was calculated to be 3.3 μm, using the following equation (14):

$$d_{ae} = d \cdot \sqrt{\rho} \quad (2)$$

where d_{ae} is the aerodynamic diameter, d is the diameter, and ρ is the particle density of mannitol, 1.48g/cm^3 (15). The FPF_{rel} enables the comparison of the dispersion efficiency between the mannitol samples.

RESULTS

Physicochemical Characterization

Jet-milled particles were produced with $d_{50\%}$ of 1.4, 2.1, 3.6, 4.8, and 10.3 μm and GSD values between 1.8 and 2.1 (Fig. 1A). Spray-dried particles were produced with $d_{50\%}$ of 1.6, 2.9, 6.6, and 7.5 μm and GSD values between 1.5 and 1.9 (Fig. 1B). Narrow size distributions were obtained with minimal overlap. Jet-milled particles were angular (Fig. 2A), whereas the spray-dried particles were spherical in shape (Figs. 2B). The size of primary particles observed by SEM was consistent with the size data obtained by laser diffraction. Varying degrees of aggregation were observed in both jet-milled and spray-dried samples, with strong aggregation observed in the smaller jet-milled samples ($d_{50\%}$ = 1.4 and 2.1 μm). All samples were highly crystalline and consisted of the same polymorphic form (beta-D-mannitol) (Fig. 3). Some peaks in the X-ray diffraction of spray-dried particles showed greatly increased relative intensities compared with the starting material. This may be explained by preferred orientation, due to both the spherical nature and the smaller particle size of the spray-dried particles compared to the starting material. The starting particles were large plates that could align in the same direction. A single sharp endothermic peak was observed around 165 to 175°C in all samples (Table I), which corresponded with the melting of mannitol (15). The onset and peak temperatures and enthalpy of fusion (ΔH) were similar for each sample. Negligible weight loss on heating was observed for each sample (Table I).

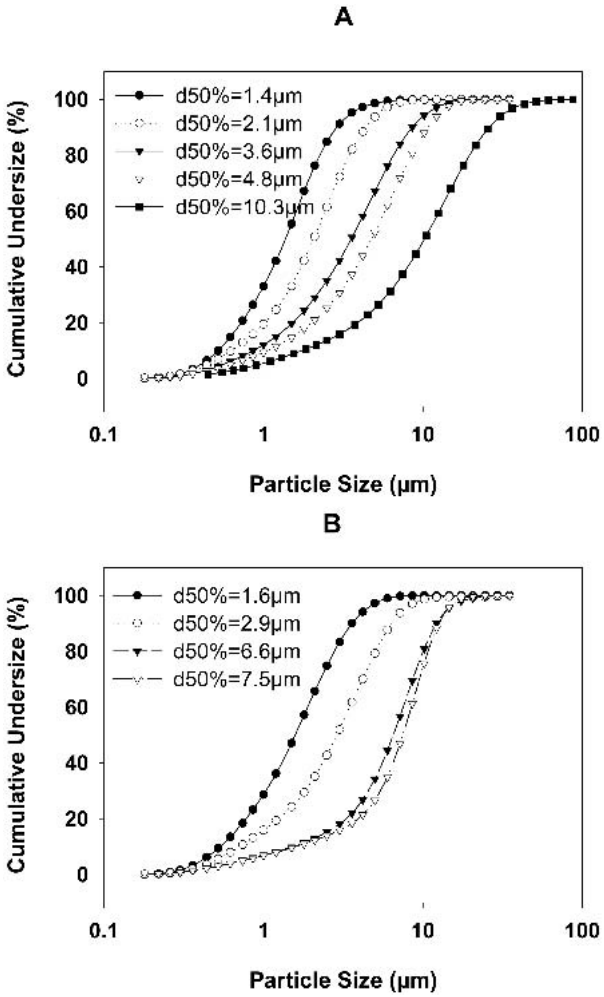

Fig. 1. Particle size distributions of (A) jet-milled and (B) spray-dried mannitol samples determined by laser diffraction using 4-bar pressure differential.

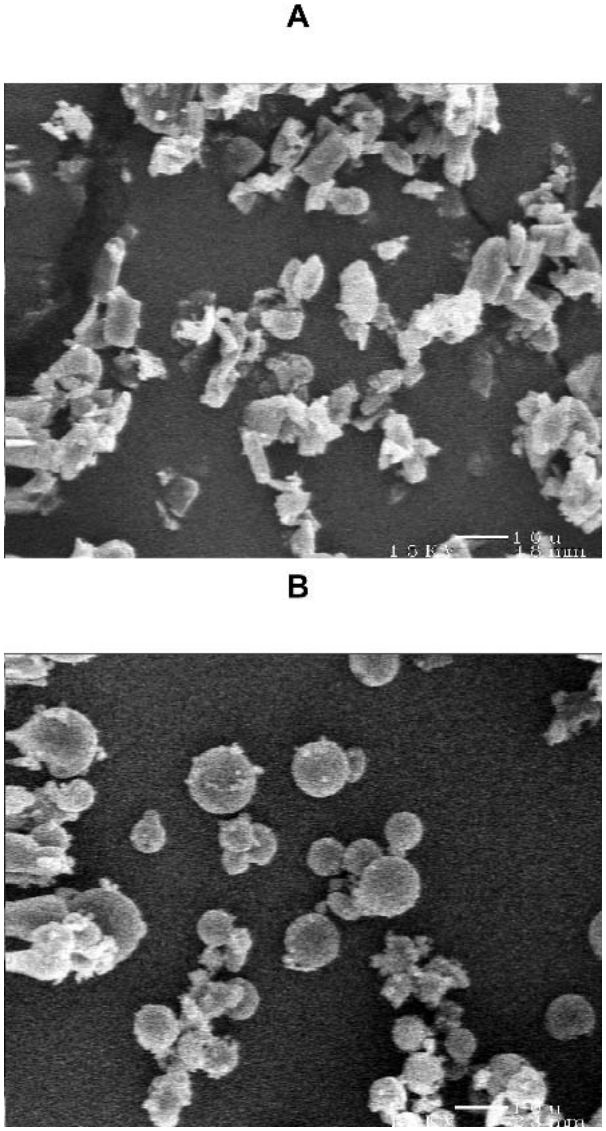

Fig. 2. Scanning electron micrographs of (A) jet-milled and (B) spray-dried mannitol samples.

Powder Flow

The bulk and tapped densities, Carr's compressibility index (CI), and fractal dimension (δ) of mannitol samples are listed in Table II. Spray-dried particles exhibited greater overall compressibility (higher CI) compared with jet-milled

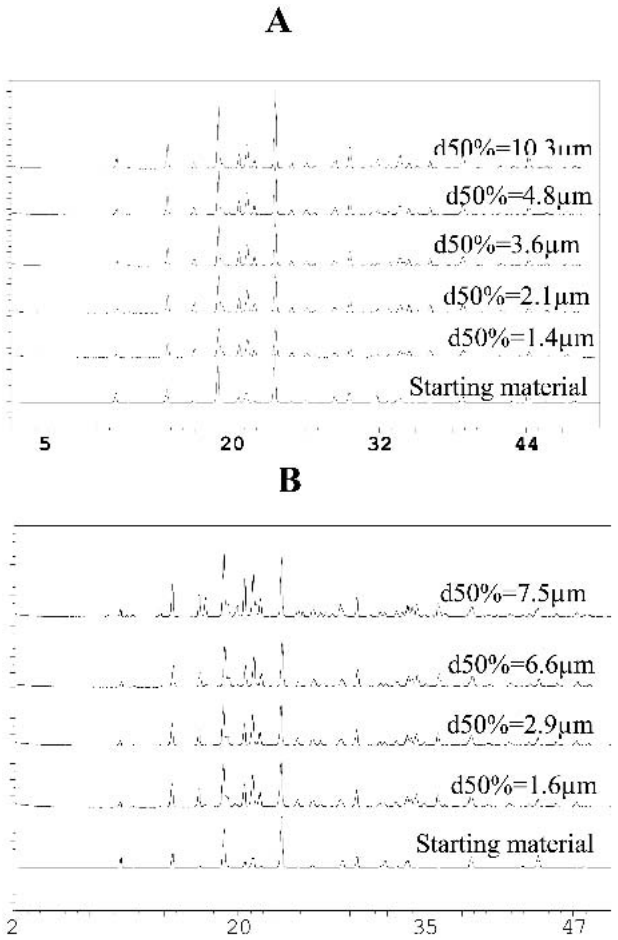

Fig. 3. Powder X-ray diffractogram of (A) jet-milled and (B) spray-dried mannitol samples.

particles. For jet-milled particles, greater compressibility (higher CI) was observed for larger particles ($d_{50\%}$ = 4.8 and 10.3 μm), whereas for spray-dried particles, greater compressibility (higher CI) was observed for both smaller ($d_{50\%}$ = 1.6 μm) and larger particles ($d_{50\%}$ = 6.6 and 7.5 μm). Significantly higher δ was obtained from the smallest spray-dried sample ($d_{50\%}$ = 1.6 μm) than all other mannitol samples ($p < 0.05$).

Aerosol Dispersion Characterization

Cascade impactions were performed at 21.5–28.0°C and 33–50% RH with the recovered dose of mannitol ranging between 84% and 115%. A summary of the data obtained from cascade impactions is presented in Table III.

Emitted Dose

Significant differences were observed in the ED of spray-dried particles due to $d_{50\%}$ using the Inhalator ($p = 0.0001$), where lower ED was obtained with smaller spray-dried particles ($d_{50\%}$ = 1.6 μm) compared with the other samples (Fig. 4). However, significant differences in ED, due to $d_{50\%}$, were not observed for spray-dried particles using the Rotahaler or for jet-milled particles using either inhaler. Significantly higher EDs ($p < 0.05$) were obtained using the Inhalator, compared with the Rotahaler, for most jet-milled and spray-dried samples. This was not true for jet-milled particles ($d_{50\%}$ = 2.1 μm) and spray-dried particles ($d_{50\%}$ = 1.6 μm).

Fine Particle Fraction

Higher overall FPFs were obtained from spray-dried particles than jet-milled particles (Fig. 5). Significant differences were observed in the FPF due to $d_{50\%}$ for jet-milled particles using both Rotahaler and Inhalator ($p < 0.05$ and $p < 0.0001$, respectively) and for spray-dried particles using both Rotahaler and Inhalator ($p < 0.0001$ each). For spray-dried particles, significantly higher FPFs were observed with smaller spray-dried particles ($d_{50\%}$ = 1.6 and 2.9 μm) than larger particles ($d_{50\%}$ = 6.6 and 7.5 μm) using both inhalers. For jet-milled particles, significantly higher FPFs were obtained with intermediate-sized jet-milled particles ($d_{50\%}$ of 2.1, 3.6, and 4.8 μm), using both inhalers. For both jet-milled and spray-dried particles, significantly higher FPF were obtained from the Inhalator, compared with the Rotahaler, except at the larger sizes.

Relative Fine Particle Fraction

Higher overall FPF_{rel}s were obtained from spray-dried particles (Fig. 6). Significant differences were observed in the FPF_{rel} due to $d_{50\%}$ for jet-milled particles using both Rotahaler and Inhalator ($p < 0.01$ and $p < 0.0001$, respectively) and for spray-dried particles using both Rotahaler and Inhalator ($p < 0.001$ and $p < 0.0005$, respectively). For jet-milled particles, significantly higher FPF_{rel}s were obtained with intermediate-sized particles ($d_{50\%}$ of 2.1, 3.6, and 4.8 μm) using both inhalers. For spray-dried particles, significantly higher FPF_{rel} was obtained with intermediate-sized particles ($d_{50\%}$ = 2.9 μm), using both inhaler devices. Significantly higher FPF_{rel}s were obtained from the Inhalator, compared with the Rotahaler ($p < 0.05$), for all jet-milled particles and the smaller spray-dried particles ($d_{50\%}$ = 1.6 and 2.9 μm) ($p < 0.05$).

Mass Median Aerodynamic Diameter

The MMAD increased with increases in $d_{50\%}$ of both jet-milled and spray-dried particles using both Rotahaler and Inhalator ($p < 0.0001$ each). Significantly smaller MMAD were obtained from the Inhalator, compared with the Ro-

Table I. Thermal Properties of Mannitol Samples Determined by Differential Scanning Calorimetry and Thermogravimetric Analysis Using a Heating Rate of 10°C/min

Sample	Onset temperature (°C)	Peak temperature (°C)	Heat of Fusion (J/g)	Weight loss on heating (%)
JM 1.4 μm	165.20	167.94	298.8	—
JM 2.1 μm	165.54	168.42	298.9	—
JM 3.6 μm	165.60	168.29	297.3	—
JM 4.8 μm	165.56	168.35	295.7	—
JM 10.3 μm	165.62	168.68	292.6	—
SD 1.6 μm	165.28	169.44	284.1	0.18
SD 2.9 μm	165.17	169.02	285.0	0.19
SD 6.6 μm	165.49	169.57	288.2	0.06
SD 7.5 μm	165.72	170.05	283.9	—

Table II. Bulk and Tapped Densities, Carr's Compressibility Index (CI), and Fractal Dimension (δ) of Mannitol Samples

Sample ($d_{50\%}$)	Bulk density (g/ml)	Tapped density (g/ml)	CI	δ*
JM 1.4 μm	0.136	0.156†	12.50	1.0315 (0.0042)
JM 2.1 μm	0.260	0.310†	14.52	1.0486 (0.0041)
JM 3.6 μm	0.246	0.322‡	23.53	1.0185 (0.0147)
JM 4.8 μm	0.292	0.398‡	31.25	1.0293 (0.0061)
JM 10.3 μm	0.413	0.487‡	30.00	1.0391 (0.0166)
SD 1.6 μm	0.297	0.426‡	30.36	1.0789 (0.0203)
SD 2.9 μm	0.346	0.475‡	27.08	1.0312 (0.0224)
SD 6.6 μm	0.382	0.572‡	33.33	1.0386 (0.0139)
SD 7.5 μm	0.369	0.602‡	38.64	1.0250 (0.0146)

‡ Determined after 5000 taps.
† Determined after 2500 taps.
* Mean value with standard deviation in parentheses, n = 3.

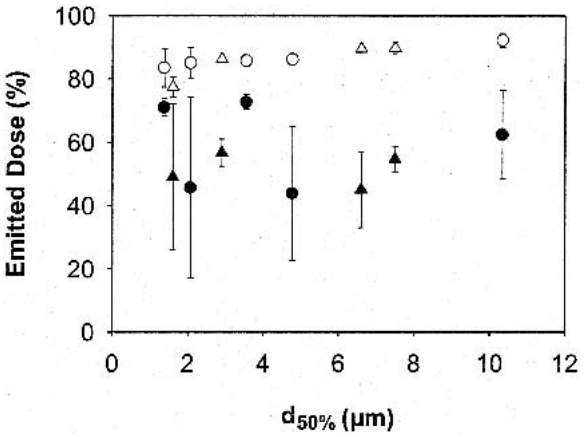

Fig. 4. Relationship between emitted dose and median diameter ($d_{50\%}$) of jet-milled and spray-dried mannitol samples (mean ± standard deviation, n = 3) where ● represents jet-milled particles dispersed using the Rotahaler, ○ represents jet-milled particles dispersed using the Inhalator, ▲ represents spray-dried particles dispersed using the Rotahaler, and △ represents spray-dried particles dispersed using the Inhalator.

tahaler for all jet-milled particles and the smaller spray-dried particles ($d_{50\%}$ = 1.6 and 2.9 μm) ($p < 0.05$).

Geometric Standard Deviation

Significant differences were observed in the GSD due to $d_{50\%}$ for jet-milled particles using both Rotahaler and Inhalator ($p < 0.001$ and $p < 0.0001$, respectively) and for spray-dried particles using both inhalers ($p < 0.0001$ each). For jet-milled particles, lower GSDs were obtained with intermediate particles ($d_{50\%}$ of 2.1, 3.6, 4.8 μm) using both inhalers. For spray-dried particles, lower GSDs were obtained with smaller particles ($d_{50\%}$ = 1.6 and 2.9 μm) using both inhalers. Minimal differences in GSD were observed due to inhaler type for both jet-milled and spray-dried particles.

DISCUSSION

Narrow size distributions of jet-milled and spray-dried mannitol particles were produced in the respirable (1–10 μm) range. The particles size ($d_{50\%}$) and particle morphology differed between the jet-milled and spray-dried particles, whereas minimal differences were observed in other physicochemical properties.

The particle size and morphology and inhaler device used significantly affected the aerosol dispersion of jet-milled and spray-dried mannitol particles. Higher FPFs and FPF_{rel}s were obtained with $d_{50\%}$ between 2 and 5 μm for both jet-milled and spray-dried particles; with lower values observed with $d_{50\%}$ closer to 1 and 10 μm. These results support a previous study where lower FPFs were observed with smaller and larger particle sizes of spray-dried mannitol and disodium cromoglycate (DSCG) particles (5, 6). Lower GSDs were observed in particles with $d_{50\%}$ between 2 and 5 μm, which was indicative of less variable aerosol dispersion; and higher GSDs were observed with $d_{50\%}$ closer to 1 and 10 μm. Higher MMADs were obtained with increasing $d_{50\%}$ for both jet-milled and spray-dried particles, which was attributed to the proportionality between aerodynamic and geometric diameters. Greater aerosol dispersion with less variation was obtained with $d_{50\%}$ between 2 and 5 μm.

Significant differences were observed between the aerosol dispersion of the angular jet-milled particles and spherical spray-dried particles. Spray-dried particles produced higher values of FPF and FPF_{rel} compared with jet-milled particles, using either inhaler device. However, differences between jet-milled and spray-dried particles were not observed in ED, MMAD, or GSD.

The specific resistances of the Rotahaler and Inhalator

Table III. Summary of Cascade Impaction Data (Mean, n = 5)

Sample ($d_{50\%}$)	ED (%)		FPF (%)		FPF_{rel} (%)		MMAD (μm)		GSD	
	Rotahaler	Inhalator	Rotahaler	Inhalator	Rotahaler	Inhalator	Rotahaler	Inhalator	Rotahaler	Inhalator
JM 1.4 μm	70.96	83.41	0.00	7.43	0.00	7.91	3.83	2.39	1.86	1.81
JM 2.1 μm	45.70	84.95	0.70	15.98	0.90	20.49	4.03	3.32	1.66	1.54
JM 3.6 μm	72.71	85.75	1.78	10.94	3.86	23.79	4.88	3.84	1.59	1.61
JM 4.8 μm	43.86	86.07	1.20	8.39	3.63	25.43	5.00	4.25	1.62	1.64
JM 10.3 μm	62.38	92.15	0.72	2.02	4.22	11.90	6.05	5.02	1.72	1.77
SD 1.6 μm	49.06	77.34	5.78	25.16	6.57	28.59	3.92	3.62	1.57	1.57
SD 2.9 μm	56.70	86.24	13.14	24.54	23.47	43.81	3.89	3.53	1.60	1.68
SD 6.6 μm	45.05	89.43	2.26	3.12	11.29	15.58	5.46	5.49	1.71	1.72
SD 7.5 μm	54.65	89.69	1.71	1.73	10.07	10.17	5.95	5.92	1.80	2.10

ED, emitted dose; FPF, fine particle fraction; MMAD, mass median aerodynamic diameter; GSD, geometric standard deviation.

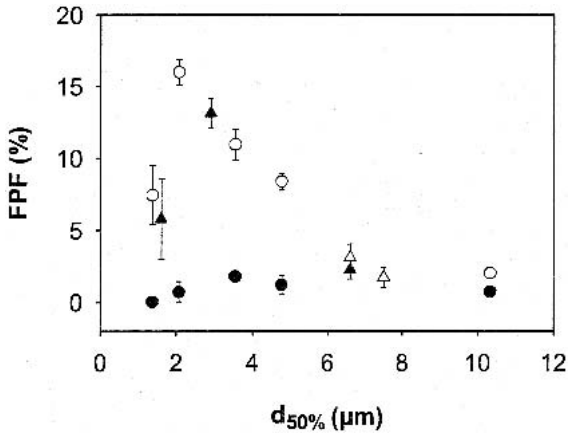

Fig. 5. Relationship between fine particle fraction (FPF) and median diameter ($d_{50\%}$) of jet-milled and spray-dried mannitol samples (mean ± standard deviation, n = 3) where ● represents jet-milled particles dispersed using the Rotahaler, ○ represents jet-milled particles dispersed using the Inhalator, ▲ represents spray-dried particles dispersed using the Rotahaler, and △ represents spray-dried particles dispersed using the Inhalator.

are 0.040 and 0.180 $cmH_2O^{1/2}$/(L/min), respectively (16). At a given flow rate, the greater pressure drop experienced using the Inhalator provides higher shear force for powder entrainment and aerosolization. Higher EDs, FPFs, and FPF_{rel}s and smaller MMADs were obtained using the Inhalator for most of the mannitol samples, as expected. In addition, the use of the Inhalator highlighted the more irregular flow (high δ value) of smallest spray-dried sample ($d_{50\%}$ = 1.6 μm), where a significantly lower ED was observed. Such differences in ED were not observed using the Rotahaler. Greater aerosol dispersion was obtained using the Inhalator, compared with the Rotahaler.

All mannitol samples flowed as aggregates, rather than discrete particles, during dynamic powder flow measurements using the vibrating spatula. The low δ values obtained for all samples indicated very regular flow properties. Particles

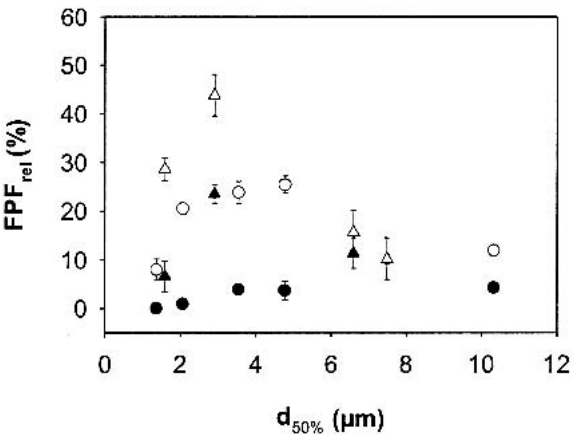

Fig. 6. Relationship between relative fine particle fraction (FPF_{rel}) and median diameter ($d_{50\%}$) of jet-milled and spray-dried mannitol samples (mean ± standard deviation, n = 3) where ● represents jet-milled particles dispersed using the Rotahaler, ○ represents jet-milled particles dispersed using the Inhalator, ▲ represents spray-dried particles dispersed using the Rotahaler, and △ represents spray-dried particles dispersed using the Inhalator.

smaller than 10 μm exhibit poor flow under gravity due to their highly cohesive nature, except as large agglomerates (17). The significantly higher δ value observed with the smallest spray-dried sample ($d_{50\%}$ = 1.6 μm) corresponded with its significantly lower ED obtained using the Inhalator. The poor aerosol entrainment of this sample was attributed to its irregular dynamic flow characteristics, suggesting that the δ values obtained using the vibrating spatula technique may provide a good estimation of ED performance and that powder entrainment occurs as aggregates from inhaler devices.

The Carr's compressibility index (CI) provided an estimation of the particle forces within the aggregates of jet-milled and spray-dried mannitol particles. CI values traditionally provide an estimate of the powder flow as discrete particles, based on the concept that compressible powders are more cohesive and exhibit poor flow. Powder flow requires individual particles to overcome the interparticulate forces in order to slide across one another. In powders exhibiting powder flow as discrete particles, higher CI values indicated that interparticulate forces were overcome during tapping with subsequent particle rearrangement increasing the bulk density. However, high CI values obtained in this study may also have resulted from the breakdown of aggregates and subsequent rearrangement of the individual particles. Particles with high interparticulate forces form stable aggregates that withstand breakdown during tapping and produce lower CI values, due to aggregate rearrangement, as observed in the smaller jet-milled particles ($d_{50\%}$ = 1.4 and 2.1 μm). Particles with weaker interparticulate forces produced higher CI values, due to the breakup of aggregates during tapping, as observed in the larger jet-milled and spray-dried samples.

Particle size and morphology influenced the powder flow behavior of jet-milled and spray-dried mannitol particles, determined by the static method where lower CI values represent better flow. Smaller jet-milled particles with strong aggregation ($d_{50\%}$ = 1.4 and 2.1 μm) exhibited excellent powder flow behavior, intermediate-sized particles (3–5-μm range) flowed well, and particle sizes closer to 1 μm and 10 μm flowed poorly. Similar observations were previously reported where particles smaller than 1 μm exhibited good fluidization as stable agglomerates, particles in the 1–5-μm range exhibited improved fluidization behavior, and particles close to 1 μm and slightly larger than 10 μm showed very poor fluidization (18).

The interparticulate forces and aggregation are important in powder flow and aerosol dispersion behavior. The transition between gravitational to thermodynamic forces occurs in the 1- to 10-μm range (19). Thermodynamic forces, exhibited as diffusional motion, predominate in particles smaller than 1 μm, and gravitational forces predominant in particles larger than 10 μm. Both forces are minimal to negligible within the 1–10-μm range, and van der Waals forces and other interparticulate forces are dominant (20,21). The magnitude of van der Waals forces increases with reducing particle size, due to reduced separation distance between particles and weaker gravitational forces. Small particles (close to 1 μm) exhibit high van der Waals forces and strong aggregation, resulting in good powder flow and entrainment but poor deaggregation during aerosol dispersion. Intermediate-sized particles (2–5 μm) exhibited weaker van der Waals forces. The loose aggregates produced exhibited good flow and entrainment properties and were easily deaggregated

within the airstream. The large particles (close to 10 μm) exhibited the weakest van der Waals forces. The deaggregation during aerosol dispersion produced large primary particles that were too large to enter the lower stages of the cascade impactor. The greater aerosol dispersion observed with spray-dried particles, compared with jet-milled particles, may be a result of their spherical shape reducing the particle contact area and van der Waals forces. Another possible reason may be the reduced electrostatic forces, associated with the method of particle generation.

This study used mannitol as a model compound for drug only powder formulations. The cohesion forces examined mimics the particle-particle interactions involved with commercial formulations containing active compounds only, without any excipients. The particulate forces involved with small drug particles and large excipient carrier particles have been examined and will be addressed in a future paper.

The effect of the width of the size distribution has not been examined in this study. Because monodisperse particles were not produced, the effect of very fine particles may play an important role in the powder flow and aerosol dispersion behavior of particles in the 1–10-μm range. Future work to be examined includes the preparation and characterization of particles with similar median diameters but varying distribution widths.

In summary, narrow distributions of mannitol particles within the respirable size (1–10 μm) were prepared using both jet-milling and spray-drying techniques. The particle size and morphology significantly affected the aerosol dispersion of jet-milled and spray-dried particles. Greater aerosol dispersion with less variation was achieved using particles with $d_{50\%}$ in the 2–5-μm range. Spray-dried particles produced greater aerosol dispersion than jet-milled particles. Small changes in the particle size within the respirable range (1–10 μm) produced a major impact in the aerosol dispersion of powders. Aggregate size and behavior appeared to play an important role in powder flow and aerosol dispersion. Greater aggregate deaggregation and subsequent aerosol dispersion was achieved with the higher resistance device (Inhalator).

ACKNOWLEDGMENTS

M. D. L. was supported by a research grant from Inhalation Product Development, GlaxoSmithKline, RTP. Brian Noga performed the X-ray diffraction analysis of samples.

REFERENCES

1. P. R. Byron. Prediction of drug residence times in regions of the human respiratory tract following aerosol inhalation. *J. Pharm. Sci.* **75**:433–438 (1986).
2. A. J. Hickey, N. M. Concessio, M. M. Van Oort, and R. M. Platz. Factors influencing the dispersion of dry powders as aerosols. *Pharm. Tech.* **8**:58–82 (1994).
3. R. J. Malcolmson and J. K. Embleton. Dry powder formulations for pulmonary delivery. *Pharm. Sci. Tech. Today.* **1**:394–398 (1998).
4. K. Masters. *Spray Drying Handbook*, Longman Scientific and Technical, New York, 1991, pp. 1–20.
5. N. Chew and H.-K. Chan. Influence of particle size, air flow and inhaler device on the dispersion of mannitol powders as aerosols. *Pharm. Res.* **16**:1098–1103 (1999).
6. N. Y. K. Chew, D. F. Bagster, and H.-K. Chan. Effect of particle size, air flow and inhaler device on the aerosolisation of disodium cromoglycate powders. *Int. J. Pharm.* **206**:75–83 (2000).
7. A. Chawla, K. M. G. Taylor, J. M. Newton, and M. C. R. Johnson. Production of spray dried salbutamol sulphate for use in dry powder aerosol formulation. *Int. J. Pharm.* **108**:233–240 (1994).
8. M. T. Vidgren, P. A. Vidgren, and T. P. Paronen. Comparison of physical and inhalation properties of spray-dried and mechanically micronized disodium cromoglycate. *Int. J. Pharm.* **35**:139–144 (1987).
9. M. D. Louey, M. M. van Oort, and A. J. Hickey. The effect of spray-drying parameters on particle size of mannitol particles. *AAPS PharmSci.* **3** (2001).
10. J. Sánchez. Colorimetric assay of alditols in complex biological samples. *J. Agr. Food Chem.* **46**:157–169 (1998).
11. A. J. Hickey and N. M. Concessio. Flow properties of selected pharmaceutical powders from a vibrating spatula. *Part. Part. Syst. Charact.* **11**:457–462 (1994).
12. T. M. Crowder and A. J. Hickey. An instrument for rapid powder flow measurement and temporal fractal analysis. *Part. Part. Sys. Charact.* **16**:32–34 (1999).
13. C. A. Dunbar, A. J. Hickey, and P. Holzner. Dispersion and characterisation of pharmaceutical dry powder aerosols. *Kona.* **16**:7–45 (1998).
14. I. Gonda. Targeting by deposition. In A.J. Hickey (ed.), *Pharmaceutical Inhalation Aerosol Technology*, Marcel Dekker, Inc., New York, 1992, pp. 61–82.
15. A. Wade and P. J. Weller. *Handbook of Pharmaceutical Excipients,* London Pharmaceutical Press, London, 1994.
16. A. R. Clark and A. M. Hollingworth. The relationship between powder inhaler resistance and peak inspiratory conditions in healthy volunteers—implications for in vitro testing. *J. Aerosol Med.* **6**:99–110 (1993).
17. J. N. Staniforth. Powder flow. In M.E. Aulton (ed.), *Pharmaceutics: The Science of Dosage Form Design*, Churchill Livingstone, New York, 1988, pp. 600–615.
18. Z. Wang, M. Kwauk, and H. Li. Fluidization of fine particles. *Chem. Eng. Sci.* **53**:377–395 (1998).
19. H. M. Jaeger, S. R. Nagel, and R. P. Behringer. The physics of granular matter. *Physics Today* **49**:32–38 (1996).
20. J. Visser. Van der Waals and other cohesive forces affecting powder fluidization. *Powder Tech.* **58**:1–10 (1989).
21. J. Visser. Particle adhesion and removal: a review. *Part. Sci. Tech.* **13**:169–196 (1995).